Journal of Molecular Liquids 426 (2025) 127352

Contents lists available at ScienceDirect

Journal of Molecular Liquids

journal homepage: www.elsevier.com/locate/molliq

Molecular insights into the motion of oil droplets in aqueous solutions of ester- and amide-containing cationic surfactants

Kazuki Ueno [a], Yuuki Ishiwatari [b], Ken Sasaki [b], Tomoya Kojima [a], Atsuro Takai [c], Kouichi Asakura [a], Noriyoshi Arai [b], Taisuke Banno [a,*]

[a] Department of Applied Chemistry, Faculty of Science and Technology, Keio University, 3-14-1 Hiyoshi, Kohoku-ku, Yokohama 223-8522, Japan
[b] Department of Mechanical Engineering, Faculty of Science and Technology, Keio University, 3-14-1 Hiyoshi, Kohoku-ku, Yokohama 223-8522, Japan
[c] Molecular Design and Function Group, National Institute for Materials Science (NIMS), 1-2-1 Sengen, Tsukuba, Ibaraki 305-0047, Japan

ARTICLE INFO

Keywords:
Self-propelled motion
Oil droplet
Cationic surfactant
Intermolecular interaction

ABSTRACT

The study of self-propelled motion in soft matter systems has garnered significant interest owing to its potential applications in microfluidics, soft robotics, and autonomous system design. Understanding the molecular mechanisms underlying motility is crucial for advancing these applications. This study investigates the self-propelled motion of lauronitrile oil droplets in aqueous surfactant solutions, focusing on the impact of different surfactant molecular structures on droplet dynamics. This study compares surfactants with ester and amide linkages, highlighting their critical role in modulating interfacial tension and driving Marangoni convection, a key factor behind droplet movement. Surfactants with ester linkages exhibit a high affinity for lauronitrile and rapidly adsorb at the oil–water interface, generating strong Marangoni flows and driving fast droplet motion. In contrast, amide-containing surfactants exhibit slower adsorption and weaker interactions with lauronitrile, leading to reduced or absent motion. These findings provide new insights into the molecular mechanisms underlying the self-propelled droplet behavior in non-equilibrium systems and contribute to a deeper understanding of self-organizing phenomena.

1. Introduction

The study of self-propelled objects is of particular interest in non-equilibrium dynamics and soft matter physics [1]. This phenomenon, characterized by the spontaneous movement of objects without an external energy supply, has a wide range of potential applications [2–8]. These include the emergence of complex self-organization phenomena from the cooperative action of biomolecules and microorganisms in nature and the design of autonomous microdevices in artificial systems. Among self-propelled objects, droplets are isotropic in shape and require symmetry breaking to realize movement [9–12]. Therefore, droplets have frequently been used as mathematical models.

Several factors control the self-propelled mechanism of droplets. In particular, the Marangoni effect, caused by the heterogeneity of the interfacial tension, has been recognized as the main driving force [13–16]. This understanding is supported by experimental evidence that the heterogeneity of interfacial tension on the droplet surface is caused by changes in the distribution of surfactants [17–19] and local accumulation of solid nanoparticles [20]. Spatial anisotropy, such as chemical gradients, also induces heterogeneity in the interfacial tension of the droplet surface [21–24]. This heterogeneity creates a driving force that causes the droplet to start moving spontaneously.

Some research groups, including ours, have investigated the influence of surfactants on the self-propelled behavior of droplets [25–28]. The effects of surfactant concentration and molecular structure on droplet movement speed and direction have been reported. In particular, discussions have focused on how surfactant adsorption on the droplet surface alters the interfacial tension, creating heterogeneity that drives self-propelled motion. However, the specific effects of different surfactant species and their molecular structures on the motion modes of oil droplets remain poorly understood. Few studies have systematically compared the self-propelled motion of droplets in aqueous solutions with different surfactants [29], highlighting the need for a deeper understanding of the interaction mechanisms between surfactants and oil droplets.

In this study, we investigated the self-propelled behavior of oil

* Corresponding author.
E-mail address: tbanno@keio.jp (T. Banno).

https://doi.org/10.1016/j.molliq.2025.127352
Received 21 November 2024; Received in revised form 25 February 2025; Accepted 8 March 2025
Available online 10 March 2025

droplets in aqueous solutions with different surfactants, focusing on how the structure of each surfactant molecule contributes to the motion modes of the oil droplets (Fig. 1). Specifically, we designed and synthesized surfactants with the ester (**Es**) and amide (**Am**) linkages between the hydrophobic and hydrophilic groups, respectively, as well as hybrid surfactants, **AmAlaEs** and **AmGlyEs**, incorporating both groups. Then, we compared the behavior of the lauronitrile droplets in these surfactant solutions. In addition, the effect of the methyl side chain in amide-ester-type surfactants on droplet dynamics was evaluated. These studies not only deepen our fundamental understanding of the mechanism of self-propelled droplets but also suggest potential future applications in the design of more efficient chemical systems exhibiting self-propelled motion and the development of microfluidic devices.

2. Materials and methods

2.1. General

Commercially available reagents and solvents were purchased from Tokyo Chemical Industry Co. (Tokyo, Japan), Wako Chemical Co. (Osaka, Japan), and Kanto Chemical Co. (Tokyo, Japan). They were used without further purification. ^{1}H NMR spectra were recorded on ECA-500 Fourier transform spectrometers (JEOL Ltd., Tokyo, Japan) at 500 MHz. Chemical shifts were calculated in parts per million (ppm) using tetramethylsilane as a standard (0 ppm). Mass spectrometry was performed by electrospray ionization using a TimsTOF instrument (Bruker, Massachusetts, USA). The synthetic procedure of cationic surfactants having ester and amide linkages is described in the Supplementary Information.

2.2. Observation of oil droplets in aqueous surfactant solution

Microscopic observations were performed to observe whether the oil droplets were self-propelled in the aqueous solution of synthesized surfactants. First, 80 μL of an aqueous surfactant solution with a concentration of 50 mM was added in a flame-sealed chamber (15 × 15 × 0.28 mm; Bio-Rad, CA). The oil component was dispersed in the surfactant solution using a Femto Jet 4i (Eppendorf Co., Hamburg, Germany); after 20 injections of the oil component with the Femto Jet, the dispersion was sealed with a glass slide (24 × 60 mm; NEO Cover Glass, Matsunami Glass Industry, Osaka, Japan). The dispersion was observed using a phase contrast microscope (BX51, Olympus Co., Tokyo, Japan) equipped with a CCD camera (DP22, Olympus Co., Tokyo, Japan), and the observed moving images were analyzed using ImageJ.

2.3. Measurement of interfacial tension

The oil–water interfacial tension was measured by the pendant drop method with a contact angle meter DMs-501 (Kyowa Kagaku Co. Ltd., Tokyo, Japan). A quartz glass cell was filled with 7.5 mL of lauronitrile, into which 0–1 mM surfactant solution was injected from a syringe to create a droplet at the needle tip. The shape of the droplet was fitted to the Young-Laplace equation to obtain the oil–water interfacial tension. Measurements were taken at 1 s intervals for 180 s at room temperature (23–25 °C).

The molecular occupied area (A_{min}) was calculated according to the Gibbs adsorption equation [30,31]. The surface excess concentration (Γ) in mol m^{-2} and the corresponding A_{min} in nm^2 at the liquid/air interface were calculated using Eqs. (1) and (2)

$$\Gamma = \frac{-1}{2.303nRT}\left(\frac{d\gamma}{d\log C}\right) \quad (1)$$

$$A_{min} = \frac{10^{20}}{N_A\Gamma} \quad (2)$$

where n is a constant that depends upon the individual ions comprising the surfactant. For cationic surfactants, the value $n = 2$ is used. The term $d\gamma/d\log C$ is the slope of the surface tension *vs* concentration curve below the critical micelle concentration (CMC) at a constant temperature, γ is the surface tension in mN m^{-1}, T is the absolute temperature, and R and N_A are the ideal gas constant and Avogadro's number, respectively.

2.4. Measurement of infrared (IR) spectra

A mixture was prepared by adding 5 μL of lauronitrile and 5 mg of surfactant (**Es**, **Am**, and **AmALaEs**) to 1 mL of chloroform and volatilizing the chloroform. IR measurements of prepared samples were performed using the KBr method with a Fourier transform infrared spectrometer ALPHA (Bruker Co., Billerica, MA). Measurements were also carried out in the solid and liquid state for the surfactant and lauronitrile alone.

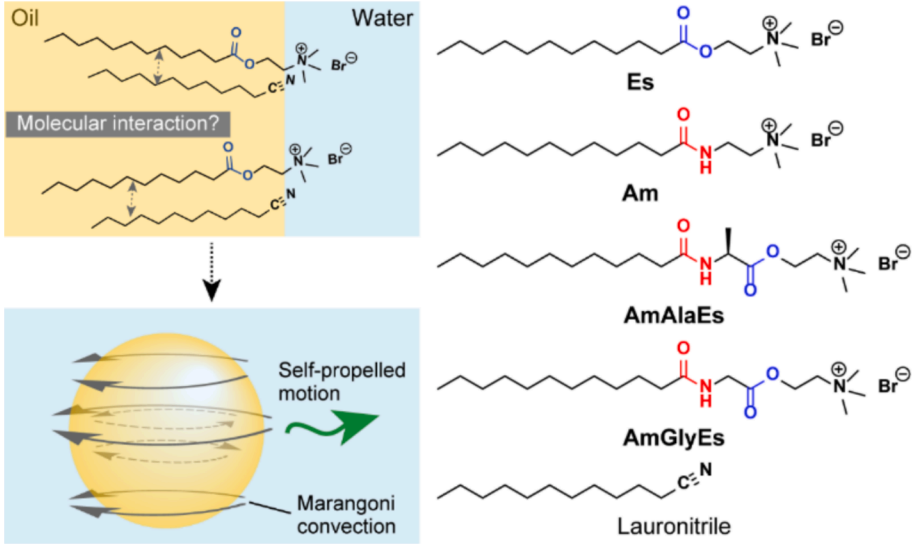

Fig. 1. Conceptual scheme of this study and molecular structures of synthesized cationic surfactants: **Es**, **Am**, **AmAlaEs** and **AmGlyEs**, and lauronitrile as an oil component.

2.5. Molecular dynamic simulations at the droplet surface

The simulations were performed using GROMACS free software package (version 2023.2) [32]. To create the initial structure, 1175 water molecules, and 98 lauronitrile molecules were randomly placed to form water and oil layers. A surfactant layer was then formed by arranging 49 surfactant molecules (**Es** or **Am**) in a 7 × 7 grid with 0.5 nm spacing. These layers were combined along the *z*-axis in the following order: water, surfactant, oil, and surfactant. The system underwent energy minimization, followed by a 0.4 ns *NVT* dynamics simulation at 298 K. Finally, a 20 ns *NPT* simulation at 298 K and 1 atm was conducted to stabilize the interface, with analysis based on the 10–20 ns period.

3. Results and discussion

3.1. Microscopic observation of oil droplets in aqueous surfactant solutions

Self-propelled motion of lauronitrile oil droplets was observed in aqueous solutions of **Es**, **AmAlaEs**, and **AmGlyEs**, but not in the **Am** solution (Fig. 2a and Movies S1–S4). In the three aqueous surfactant solutions where self-propelled motion occurred, the speed of droplet movement increased with droplet size in the range of 10–150 μm (Fig. 2b). The typical lifetime for self-propelled droplets was 30 min because they vanished within this time. To compare the difference in the initial motion speed of droplets with the surfactant species, we analyzed the motion speed of five oil droplets with a diameter of 40–60 μm immediately after and 2 min after the start of observations using ImageJ. The motion speed was approximately 150 μm/s and almost did not vary for the analyzed period in the **Es** solution. Meanwhile, the speed was 70 μm/s immediately after the start of observation and became slower in

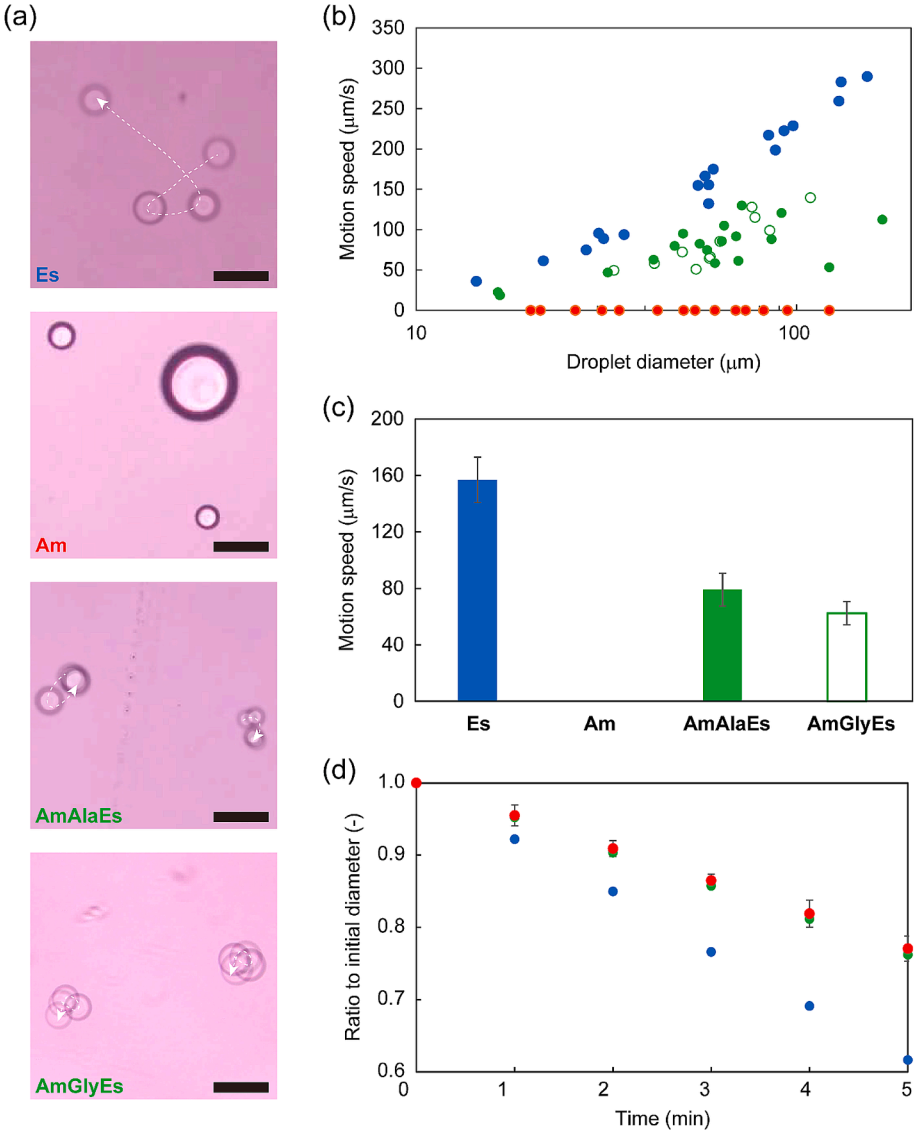

Fig. 2. Motion modes of lauronitrile droplets in an aqueous surfactant solution. (a) Sequential micrographs of droplets in **Es**, **Am**, **AmAlaEs** and **AmGlyEs** solutions. White arrows indicate the trajectory of the self-propelled droplets. The time interval between each droplet is 1 s. Scale bar: 100 μm. (b) Motion speed of droplets depending on their diameter when using **Es** (blue), **Am** (red), **AmAlaEs** (closed green), and **AmGlyEs** (open green). (c) Motion speed of droplets with a diameter of 40–60 μm in a surfactant solution. $N = 5$. (d) Time course of the droplet diameter when using **Es** (blue), **Am** (red), and **AmAlaEs** (green). The ratio of the droplet diameter was calculated using ImageJ. $N = 5$. (For interpretation of the references to colour in this figure legend, the reader is referred to the web version of this article.)

the **AmAlaEs** solution (Fig. S1). In the **AmGlyEs** solution, the initial speed was also 70 μm/s, which exhibited no significant difference based on the *t*-test between **AmGlyEs** and **AmAlaEs** ($p > 0.05$) (Fig. 2c). The methyl side groups did not significantly affect the speed of motion of the oil droplets. Therefore, further experiments were conducted to compare the motion modes of lauronitrile droplets in the **Es**, **Am**, and **AmAlaEs** solutions.

We investigated whether the variation in motion speed across different surfactants was related to the solubilization rate at which the oil was incorporated into the micelles. During solubilization, empty micelles in the aqueous phase collided with oil droplets, and the solubilized oil components were released into the bulk aqueous phase. This induced anisotropy on the oil droplet surface, resulting in the self-propelled motion of droplets [12]. Several research groups have identified characteristic phenomena, such as the transfer of oil components into empty micelles, leading to the collective motion of multiple droplets due to surface anisotropy [33,34], or the avoidance of oil-filled swollen micelles [35]. Therefore, the rate at which the oil droplet size changes in each aqueous surfactant solution was analyzed as the solubilization rate. One oil droplet was traced for 5 min, and its size was analyzed every minute. In all aqueous surfactant solutions, the oil droplets gradually decreased in size during the observation period, particularly in the **Es** solution. The speed of movement correlated directly with the rate of solubilization; faster movement resulted in quicker solubilization. On the other hand, the oil droplets became smaller in the **Am** solution, where no droplet motion was observed, at the same rate as that in the **AmAlaEs** solution, where self-propelled motion was observed (Fig. 2d). These results suggested that only the solubilization of oil components was not the dominant factor for the motion speed of oil droplets.

3.2. Comparison of Marangoni convection in different surfactant solutions based on measurements of the interfacial tension

Because the self-propelled motion of oil droplets is due to Marangoni convection generated by the heterogeneity of the interfacial tension, the difference in local interfacial tension at the oil droplet surface is related to the motion speed. Therefore, oil–water interfacial tension measurements were performed using the pendant drop method. A surfactant solution was ejected from the needle tip of the syringe and the interfacial tension was determined from the shape of the droplet by fitting it to the Young–Laplace equation. At a surfactant concentration of 0.1 mM, the interfacial tension remained consistent during the measurement time for any surfactant. On the other hand, at surfactant concentrations of 0.5 and 1.0 mM, **AmAlaEs** and **Am** took approximately 150 s to reach a constant value, whereas **Es** reached a constant value within 30 s (Fig. 3a1–3). The constant value was defined as the point at which the change in the interfacial tension for 10 s was less than 0.1 mN/m. The results indicated that **Es** adsorbed on the surface of lauronitrile droplets faster than **AmAlaEs** and **Am**, suggesting that the faster the surfactant adsorbs on the droplet surface, the quicker solubilization occurred. This resulted in faster motion of the droplets in the **Es** solution. The relatively slow adsorption of **AmAlaEs** and **Am** was probably due to the higher affinity between the amide linkages and water.

The concentration dependence of the interfacial tension at surfactant

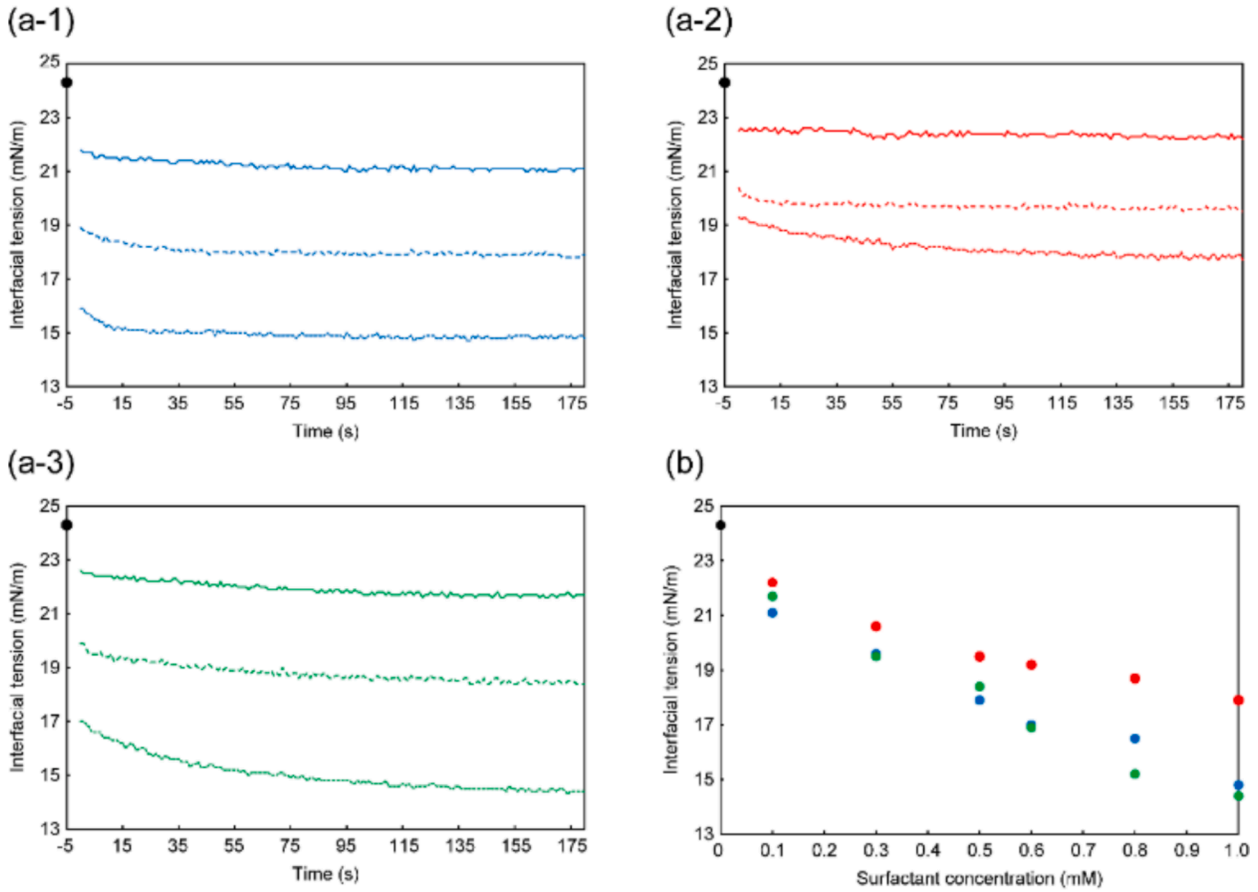

Fig. 3. Interfacial tension between the aqueous surfactant solution and lauronitrile according to the pendant drop method at room temperature (23–25 °C). (a) Time-dependent change in the interfacial tension using **Es** (a-1), **Am** (a-2), and **AmAlaEs** (a-3). The measurements started 5 s after the water droplet was prepared in the oil through a syringe. The surfactant concentrations were 0.1 (solid line), 0.5 (dashed line), and 1 mM (dotted line). (b) The relationship between the surfactant concentration and interfacial tension: **Es** (blue), **Am** (red), and **AmAlaEs** (green). The black circles in each panel indicate the interfacial tension between water and lauronitrile. (For interpretation of the references to colour in this figure legend, the reader is referred to the web version of this article.)

concentrations between 0 and 1 mM was investigated. A comparison of the interfacial tension after 180 s at each concentration showed that the interfacial tension decreased with increasing surfactant concentration for all surfactants. Significantly, the concentration dependence of **Am** was less than those of **Es** and **AmAlaEs** (Fig. 3b). The oil–water interfacial tension is related to the intermolecular interactions between oil, water, and surfactant molecules, such as the dispersion force between the hydrophobic groups and hydration of the polar groups of the surfactant and oil molecules. Therefore, the intermolecular interactions between lauronitrile and **Es**, as well as between lauronitrile and

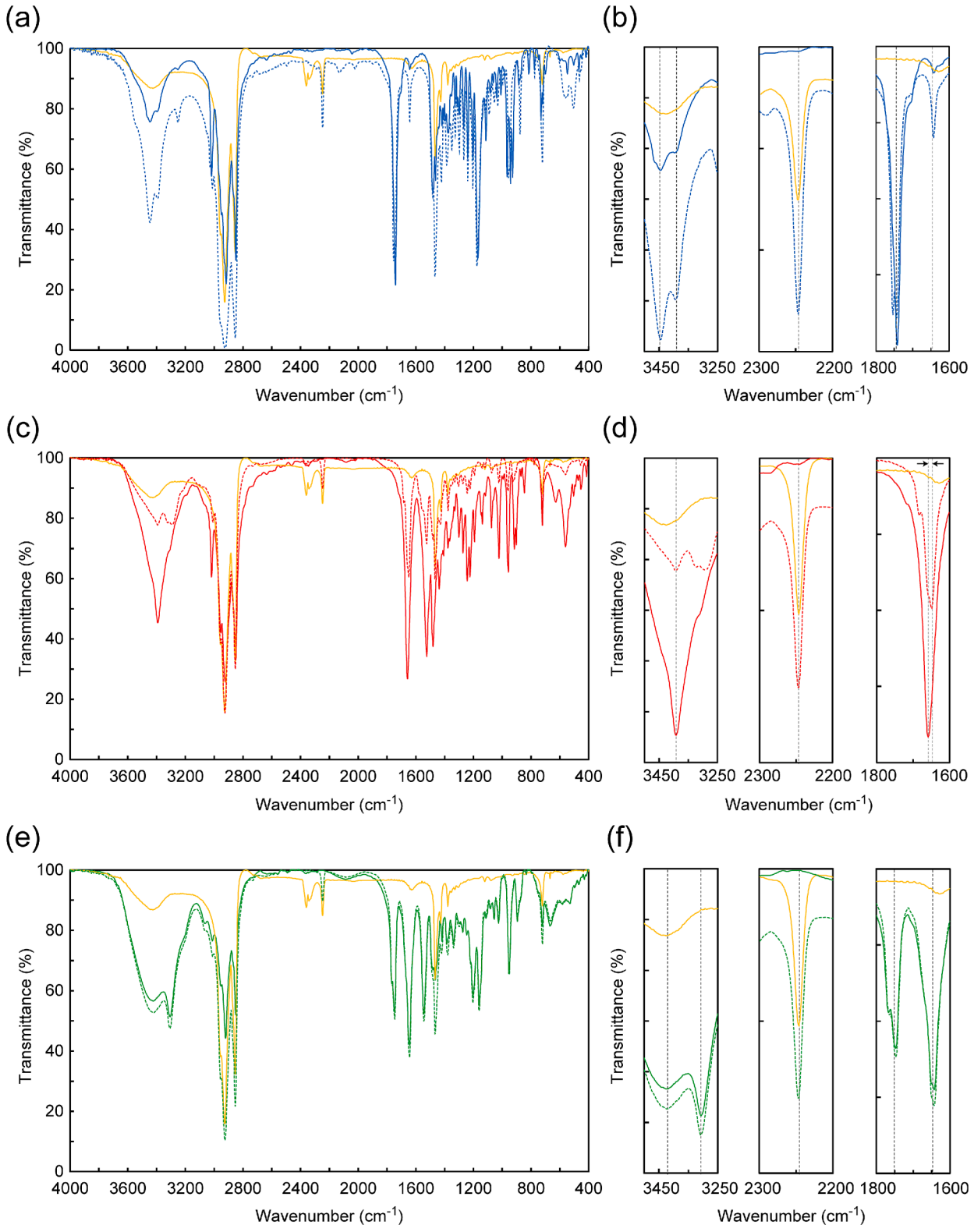

Fig. 4. Infrared spectra of (a,b) **Es**, (c, d) **Am**, and (e, f) **AmAlaEs** (solid lines), lauronitrile (solid orange lines), and their mixtures (dotted lines). The arrows in panel (d) indicate a shift of the wavenumber. (For interpretation of the references to colour in this figure legend, the reader is referred to the web version of this article.)

AmAlaEs, were stronger than those between **Am** and lauronitrile. The significant difference in the interfacial tension, that is, the high concentration dependence on the surfactant concentration, suggested a strong Marangoni convection at the oil droplet surface. Recent predictions from coarse-grained dissipative particle dynamics simulations suggested that stronger Marangoni convection leads to faster movement of the oil droplet [36]. **Es** and **AmAlaEs** experience strong Marangoni convection because they lower the interfacial tension in a small concentration range. As a result, the lauronitrile droplets moved more in these aqueous solutions than in the **Am** solutions. These considerations are based on a perspective that links the microscopic interactions between the oil, water, and surfactant molecules with the macroscopic motion of the droplets.

3.3. Estimation of interactions between surfactants and lauronitrile at the droplet surface

The results of the oil–water interfacial tension measurements suggested differences in the oil–water–surfactant molecular interactions depending on the type of surfactant. IR spectroscopy measurements of a mixture of surfactants and lauronitrile were performed to further investigate the details using **Es**, **Am**, and **AmAlaEs**. Measurements were also performed for the pristine surfactant and lauronitrile. Peaks derived from quaternary ammonium salts in **Es** were detected at 3500–3300 cm^{-1}, carbonyl groups (C=O) at 1743 cm^{-1}, and stretching vibrations of cyano groups (CN) in lauronitrile at 2246 cm^{-1} (Fig. 4a). In the mixture of **Es** and lauronitrile, the peaks from the carbonyl groups split into two, suggesting an interaction between **Es** and lauronitrile. However, no apparent shift was observed for the cyano group peak. For **Am**, the peak derived from the C=O stretching vibration of the amide linkage in **Am** showed a lower wavenumber shift from 1658 to 1649 cm^{-1} in the mixture with lauronitrile. No peak shift for the cyano group was observed in this mixture, suggesting that neither the amide linkage nor the quaternary ammonium salt group interacted with lauronitrile. Although it was difficult to confirm the shift in the NH peak owing to the overlap with peaks from quaternary ammonium salts, these results suggested stronger hydrogen bonds between **Am** molecules at the oil droplet surface compared to those formed when **Am** molecules are not at the droplet surface. For **AmAlaEs** and lauronitrile, there was no significant shift in the wavenumber of the C=O groups in either the amide or ester linkages or CN in the cyano group upon mixing them. This indicated that there were no clear interactions between the polar groups of **AmAlaEs** and lauronitrile. These results suggested that **Es** and **AmAlaEs** mainly interacted with lauronitrile because of the dispersion force on the droplet surface, resulting in stronger intermolecular interactions than those between **Am** and lauronitrile.

To compare the adsorption modes of the **Es**, **Am**, and **AmAlaEs** molecules at the oil–water interface, their A_{min} values were calculated and compared using the Gibbs adsorption isotherm equation based on the relationship between the oil–water interfacial tension and surfactant concentration. As surfactants have an affinity for both the aqueous and oil phases, surfactant molecules at the oil–water interface have a lower degree of orientation than those at the air–water interface. Therefore, the A_{min} at the oil–water interface generally tends to be larger. Using this characteristic, the ratio of the A_{min} values of **Es** and **Am** molecules at the oil–water and air–water interfaces was determined, and the differences in adsorption modes at the oil–water interface were investigated. As shown in Figs. 5 and S1, the excess adsorption per unit area (Γ) of **Es** molecules was calculated using the slope. Then, the A_{min} was determined as the reciprocal of Γ. As shown in Table 1, among the tested surfactants, the ratio of A_{min} value of **Am** at the oil–water interface was smaller than that of **Es** and **AmAlaEs** This indicated that **Am** molecules showed a high orientation when adsorbed on the surface of the lauronitrile oil droplets, suggesting relatively strong interactions between **Am** molecules, particularly the formation of hydrogen bonds.

Molecular dynamics simulations were also performed to predict the interactions between surfactants and oil molecules or between surfactants at the oil droplet surface (Fig. 6a and b). The number of molecules was determined based on previous studies [37–39]. Considering changes in the interfacial area under the *NPT* ensemble, the number of surfactant molecules at the oil–water interface was set to 49. However, since two surfactant layers were placed in the system in this simulation, the total number of surfactant molecules was 98. The simulation involved the calculation of radial distribution functions ($g(r)$), which is a process executed with precision. No clear interaction peaks were observed between the nitrogen atom of lauronitrile and carbonyl oxygen atoms of **Es** or **Am**, and no significant differences were observed in their interactions (Fig. 6c). In the small r region, the oxygen atoms in the surfactant molecules were sandwiched between the carbon chain layer and the

Table 1
Molecular occupied areas (A_{min}) of synthesized cationic surfactants.

Surfactant	A_{min} at the oil–water interface (10^{-20} m^2/molecule)*	A_{min} at the air–water interface (10^{-20} m^2/molecule)*	Ratio of oil–water to air–water
Es	147	53	2.8
Am	119	58	2.0
AmAlaEs	205	73	2.8

* Calculated using Gibbs adsorption equation (see Experimental section).

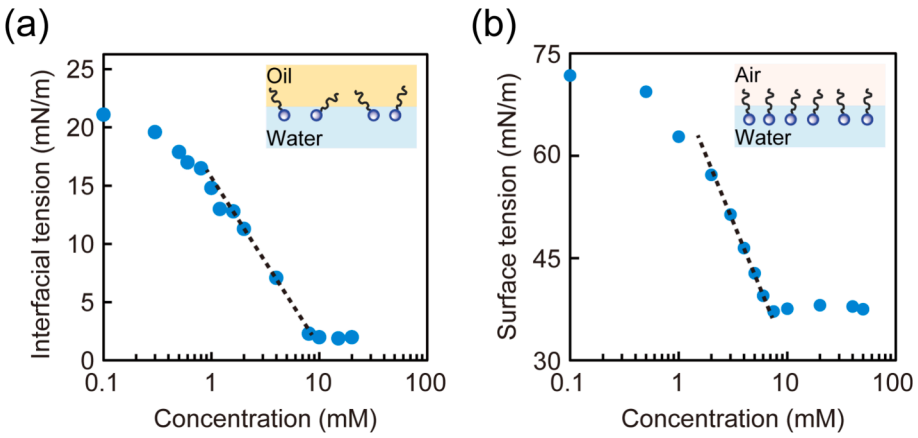

Fig. 5. (a) Interfacial and (b) surface tensions depending on the concentration of **Es** measured by the pendant drop method at room temperature. The dotted lines indicate the approximate straight line below the critical micelle concentration of **Es**. Insets indicate the schematic illustration for the adsorption of surfactant molecules at the (a) oil–water and (b) air–water interfaces.

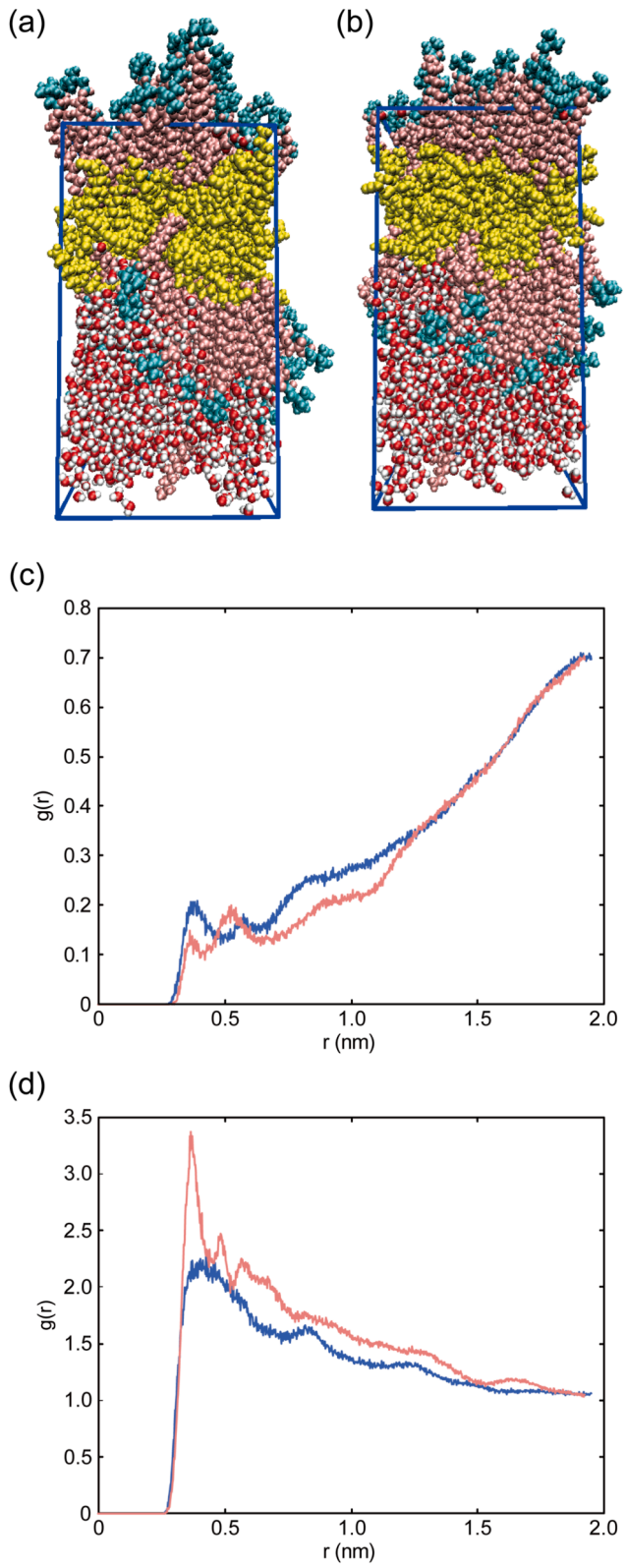

Fig. 6. Molecular dynamics (MD) snapshots for water/oil interface systems of (a) **Es** and (b) **Am**. Surfactants: the light blue and purple beads; lauronitrile: yellow beads; water: the red and white beads. (c) Radial distribution functions from the centre of mass position between oil molecules in **Es** (blue) and **Am** (red) surfactant systems, respectively. (d) Radial distribution functions between the oxygen atoms in the ester and amide linkages of **Es** (blue) and **Am** (red), respectively. (For interpretation of the references to colour in this figure legend, the reader is referred to the web version of this article.)

water molecule layer. This reduced the probability of finding nitrogen atoms in lauronitrile near the oxygen atoms in the surfactant molecules, resulting in $g(r)$ values below 1.0. The $g(r)$ value gradually approached 1.0 with increasing r. On the other hand, a comparison of $g(r)$ with the distance between the carbonyl oxygen atoms in the surfactant molecules showed that the $g(r)$ between **Am** molecules was more significant than that between **Es** molecules, confirming a strong interaction between **Am** molecules (Fig. 6d). This result strongly supported the formation of hydrogen bonds between **Am** molecules adsorbed on the oil droplet surface.

3.4. Proposed mechanism for the different motion modes of oil droplets

Based on the above considerations, the differences in the motion modes of the lauronitrile droplets due to the different surfactant species could be estimated (Fig. 7). The two key factors are considered to be associated with the motion speed of oil droplets: the interfacial tension gradient at the droplet surface and the solubilization rate. First, **Es** molecules have a relatively high affinity for lauronitrile molecules because of the dispersion forces between their hydrophobic groups. This causes a large interfacial tension difference, even for slight differences in the amount of adsorbed surfactant. Furthermore, the rapid adsorption of **Es** molecules onto the surface of the oil droplet facilitates heterogeneity in the interfacial tension due to the quicker solubilization into micelles, resulting in a strong Marangoni flow. Therefore, the large interfacial tension gradient at the droplet surface and quick solubilization enable the oil droplets to move at high speeds in the **Es** solution. On the other hand, although **Am** molecules strongly interact with each other via hydrogen bonding, their affinity for lauronitrile molecules is low, resulting in a slight difference in the interfacial tension on the droplet surface owing to differences in adsorption. Furthermore, solute–solvent interactions significantly decrease the diffusion coefficients of solutes in solvents [40,41]. Therefore, the presence of amide linkages results in a higher affinity for water molecules, which slows their diffusion in water and delays their adsorption on the oil droplet surface. This indicates slower solubilization. As a result, Marangoni convection is less likely to occur, and oil droplets are unlikely to move in the **Am** solution. Finally, **AmAlaEs** molecules have an affinity for lauronitrile molecules as high as that of **Es** molecules, and the interfacial tension tends to decrease with the amount of surfactant adsorbed. However, because they contain amide linkages, their adsorption on the oil droplet surface is delayed, resulting in slower solubilization. Therefore, it is assumed that the oil droplets do not move as fast in the **AmAlaEs** solution as in the **Es** solution due to a lower Marangoni convection strength. In addition, there is a significant decrease in motion speed over time, particularly in the **AmAlaEs** solution. The decrease in self-propelled speed with reducing droplet size may be attributed to the higher surfactant concentration at the interface, which lowers the Marangoni driving force.

The discovery of self-propelled objects driven by Marangoni convection, a phenomenon caused by the amplification of stochastic fluctuations due to slight differences in interfacial tension and the formation of large-scale convection, is a significant contribution. In this study, the use of surfactants with different properties revealed that these molecular interactions played a crucial role in the growth of fluctuations, leading to the formation of Marangoni convection and the determination of its strength. This finding suggests that molecular properties may control the macroscopic self-organising phenomena emergent in non-equilibrium systems, specifically motility. Therefore, this study provides a new perspective on molecular chemistry and is of great significance for sparking further curiosity and exploration in this field.

4. Conclusions

This study offers significant insight into the molecular mechanisms that induce the self-propelled motion of lauronitrile oil droplets in aqueous surfactant solutions. By systematically comparing the behavior

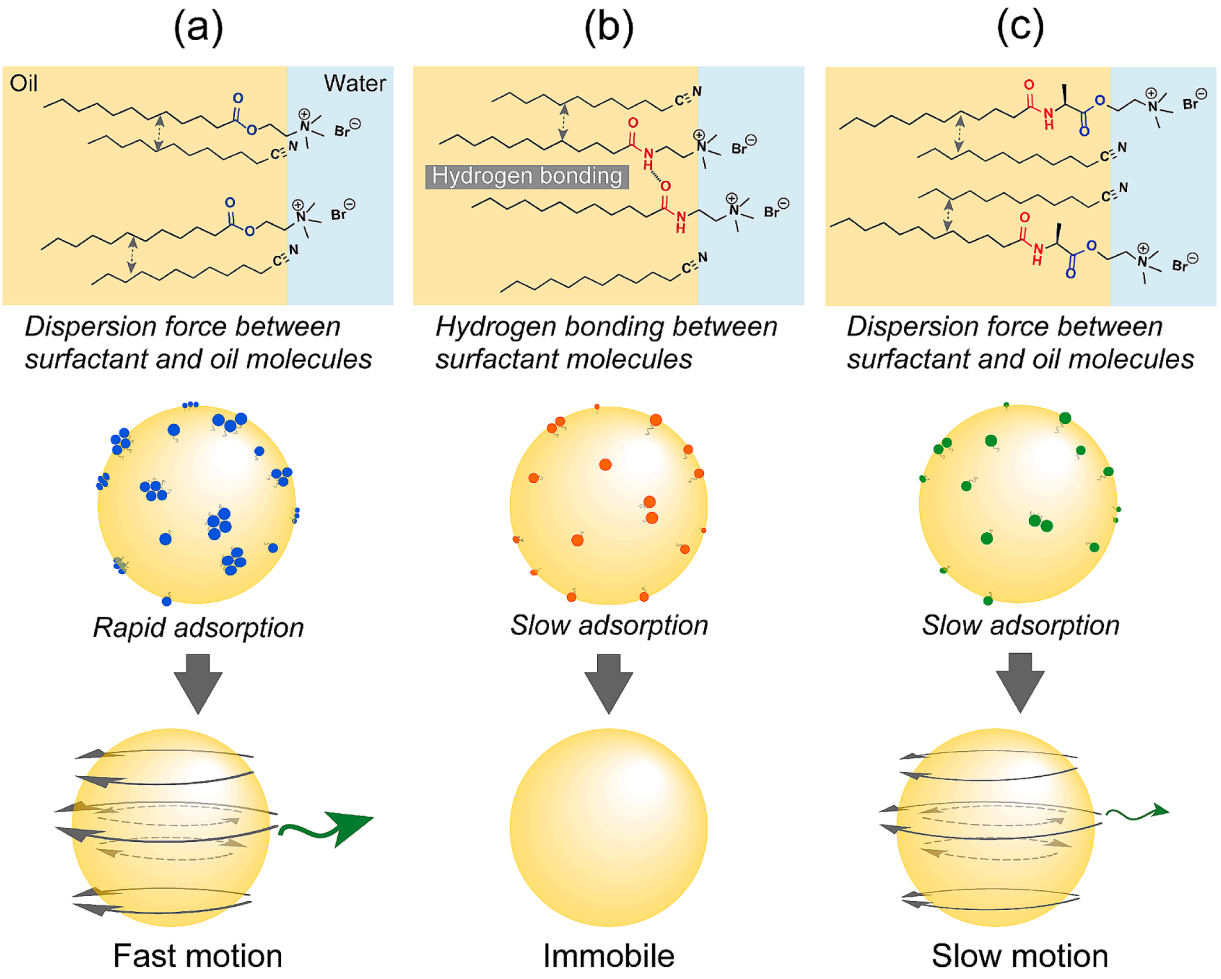

Fig. 7. Schematic illustration of differences in the motion modes of oil droplets in (a) **Es**, (b) **Am**, and (c) **AmAlaEs** solutions. The dotted two-way arrows indicate the dispersion force between oil and surfactant molecules.

of droplets in solutions containing surfactants with different molecular structures, we demonstrated that the presence of polar linkages, such as ester and amide linkages, played a crucial role in modulating the interfacial tension, thereby influencing the Marangoni convection that propels the droplets. Our results indicate that surfactants with ester linkages promoted faster droplet movement owing to their higher affinity for lauronitrile and more rapid adsorption at the oil–water interface, which generated stronger Marangoni flows. In contrast, amide-containing surfactants exhibited slower adsorption and weaker interactions with lauronitrile, resulting in diminished or no droplet movement. These findings suggest that molecular-level interactions between surfactants and oil components were key to understanding and potentially controlling macroscopic self-organization phenomena in non-equilibrium systems. These insights not only deepen our understanding of self-propelled droplets but also open new avenues for designing advanced materials and devices that leverage self-propelled motion, particularly in microfluidic and soft robotics applications. Future research could explore the application of these principles in more complex systems, potentially leading to the development of innovative autonomous microdevices and enhanced chemical systems.

CRediT authorship contribution statement

Kazuki Ueno: Writing – original draft, Methodology, Investigation, Data curation, Conceptualization. **Yuuki Ishiwatari:** Methodology, Investigation, Data curation. **Ken Sasaki:** Methodology, Investigation, Data curation. **Tomoya Kojima:** Writing – original draft, Investigation. **Atsuro Takai:** Writing – review & editing, Formal analysis, Conceptualization. **Kouichi Asakura:** Writing – review & editing. **Noriyoshi Arai:** Writing – review & editing, Validation, Methodology, Investigation, Data curation. **Taisuke Banno:** Writing – review & editing, Supervision, Methodology, Funding acquisition, Conceptualization.

Declaration of competing interest

The authors declare that they have no known competing financial interests or personal relationships that could have appeared to influence the work reported in this paper.

Acknowledgements

This study was supported by the Exploratory Research Promotion Fund from Keio Leading-Edge Laboratory of Science and Technology. This was also partially supported by JSPS KAKENHI (Grant No. JP20H02712) and JSPS Japan–Hungary Bilateral Joint Research Project (JPJSBP120213801).

Appendix A. Supplementary data

Supplementary data to this article can be found online at https://doi.org/10.1016/j.molliq.2025.127352.

Data availability

Data will be made available on request.

References

[1] Nakata, V. Pimienta, I. Lagzi, H. Kitahata, N.J. Suematsu, Self-organized Motion: Physicochemical Design based on Nonlinear Dynamics, The Royal Society of Chemistry, Cambridge, UK, 2018.

[2] S. Ghosh, A. Somasundar, A. Sen, Enzymes as active matter, Annu. Rev. Condens. Matter Phys. 12 (2021) 177–200.

[3] X. Zhao, K. Gentile, F. Mohojerani, A. Sen, Powering motion with enzymes, Acc. Chem. Res. 51 (2018) 2373–2381.

[4] Y. Tu, F. Peng, D.A. Wilson, Motion manipulation of micro-and nanomotors, Adv. Mater. 29 (2017) 1701970.

[5] J. Li, B.-E.-F. de Ávila, W. Gao, L. Zhang, J. Wang, Micro/nanorobots for biomedicine: Delivery, surgery, sensing, and detoxification, Sci. Rob. 2 (2017) eaam6431.

[6] S. Sanchez, L. Soler, J. Katuri, Chemically powered micro-and nanomotors, Angew. Chem. Int. Ed. 54 (2015) 1414–1444.

[7] N.J. Suematsu, S. Nakata, Evolution of self-propelled objects: from the viewpoint of nonlinear science, Chem. Eur. J. 24 (2018) 6308–6324.

[8] M. Fu, T. Burkart, I. Maryshev, H.G. Franquelim, A.M. Salomón, M.R. López, E. Frey, P. Schwille, Mechanochemical feedback loop drives persistent motion of liposomes, Nat. Phys. 19 (8) (2023) 1211–1218, https://doi.org/10.1038/s41567-023-02058-8.

[9] D. Babu, N. Katsonis, F. Lancia, R. Plamont, A. Ryanchun, Motile behaviour of droplets in lipid systems, Nat. Rev. Chem. 6 (2022) 377–388.

[10] S. Song, A.F. Mason, R.A.J. Post, M. De Corato, R. Mestre, A.N. Yewdall, S. Cao, R. W. van der Hofstad, S. Sanchez, L.K.E.A. Abdelmohsen, J.C.M. van Hest, Engineering transient dynamics of artificial cells by stochastic distribution of enzymes, Nat. Commun. 12 (2021) 6897.

[11] T. Banno, K. Ueno, T. Kojima, K. Asakura, Induction for self-propelled motion of artificial objects with/without shape anisotropy, J. Oleo Sci. 73 (2024) 509–518.

[12] S. Herminghaus, C.C. Maass, C. Krüger, S. Thutupalli, L. Goehring, C. Bahr, Interfacial mechanisms in active emulsions, Soft Matter 10 (2014) 7008–7022.

[13] S. Yabunaka, T. Ohta, N. Yoshinaga, Self-propelled motion of a fluid droplet under chemical reaction, J. Chem. Phys. 136 (2012) 074904.

[14] N. Yoshinaga, K.H. Nagai, Y. Sumino, H. Kitahata, Drift instability in the motion of a fluid droplet with a chemically reactive surface driven by Marangoni flow, Phys. Rev. E 86 (2012) 016108.

[15] N. Yoshinaga, Spontaneous motion and deformation of a self-propelled droplet, Phys. Rev. E 89 (2014) 012913.

[16] N. Yoshinaga, Simple models of self-propelled colloids and liquid drops: from individual motion to collective behaviors, J. Phys. Soc. Jpn. 86 (2017) 101009.

[17] A. Diguet, R. Guillermic, N. Magome, A. Saint-Jalmes, Y. Chen, K. Yoshikawa, D. Baigl, Photomanipulation of a droplet by the chromocapillary effect, Angew. Chem. Int. Ed. 48 (2009) 9281–9284.

[18] K. Suzuki, T. Sugawara, Phototaxis of oil droplets comprising a caged fatty acid tightly linked to internal convection, ChemPhysChem 17 (2016) 2300–2303.

[19] T. Kojima, H. Kitahata, K. Asakura, T. Banno, Photoinduced collective motion of oil droplets and concurrent pattern formation in surfactant solution, Cell Rep. Phys. Sci. 4 (2023) 101222.

[20] S. Cheon, L. Silva, A. Khair, L.D. Zarzar, Interfacially-adsorbed particles enhance the self-propulsion of oil droplets in aqueous surfactant, Soft Matter 17 (2021) 6742–6755.

[21] T. Ban, K. Tani, H. Nakata, Y. Okano, Self-propelled droplets for extracting rare-earth metal ions, Soft Matter 10 (2014) 6316–6320.

[22] J. Céjková, M. Novák, F. Štěpánek, M.M. Hanczyc, Dynamics of chemotactic droplets in salt concentration gradients, Langmuir 30 (2014) 11937–11944.

[23] C. Jin, C. Krüger, C.C. Maass, Chemotaxis and autochemotaxis of self-propelling droplet swimmers, PNAS 114 (2017) 5089–5094.

[24] S. Nakayama, T. Kojima, M. Kaburagi, T. Kikuchi, K. Asakura, T. Banno, Chemotaxis of oil droplets and their phase transition to aggregates with membrane structures in surfactant solution containing metal salts, ChemSystemsChem 4 (2022) e202100035.

[25] N. Ueno, T. Banno, A. Asami, Y. Kazayama, Y. Morimoto, T. Osaki, S. Takeuchi, H. Kitahata, T. Toyota, Self-propelled motion of monodisperse underwater oil droplets formed by a microfluidic device, Langmuir 33 (2017) 5393–5397.

[26] Y. Kasuo, H. Kitahata, Y. Koyano, M. Takinoue, K. Asakura, T. Banno, Start of micrometer-sized oil droplet motion through generation of surfactants, Langmuir 35 (2019) 13351–13355.

[27] D. Babu, R.J.H. Scanes, R. Plamont, A. Ryabchun, F. Lancia, T. Kudernac, S. P. Fletcher, N. Katsonis, Acceleration of lipid reproduction by emergence of microscopic motion, Nat. Commun. 12 (2021) 2959.

[28] P.J. de Visser, D. Karagrigoriou, A.-D.-C. Nguindjel, P.A. Korevaar, Quorum sensing in emulsion droplet swarms driven by a surfactant competition system, Adv. Sci. 11 (2024) 2307919.

[29] A. Hirono, T. Toyota, K. Asakura, T. Banno, Locomotion mode of micrometer-sized oil droplets in solutions of cationic surfactants having ester or ether linkages, Langmuir 34 (2018) 7821–7826.

[30] K. Esumi, K. Taguma, Y. Koide, Adsorption and micelle formation of mixed surfactant systems in water II: a combination of cationic gemini-type surfactant with MEGA-10, Langmuir 12 (1996) 4039–4041.

[31] A. Pinazo, M. Diz, C. Solans, M.A. Pés, P. Erra, M.R. Infante, Synthesis and properties of cationic surfactants containing a disulfide bond, J. Am. Oil Chem. Soc. 70 (1993) 37–42.

[32] M. Abraham, A. Alekseenko, C. Bergh, C. Blau, E. Briand, M. Doijade, S. Fleischmann, V. Gapsys, G. Garg, S. Gorelov, G. Gouaillardet, A. Gray, M. E. Irrgang, F. Jalalypour, J. Jordan, C. Junghans, P. Kanduri, S. Keller, C. Kutzner, J. A. Lemkul, M. Lundborg, P. Merz, V. Miletić, D. Morozov, S. Páll, R. Schulz, M. Shirts, A. Shvetsov, B. Soproni, D. van der Spoel, P. Turner, C. Uphoff, A. Villa, S. Wingbermühle, A. Zhmurov, P. Bauer, B. Hess and E. Lindahl, GROMACS 2023.2 Manual, Zenodo (2023). https://doi.org/10.5281/zenodo.8134388.

[33] C.H. Meredith, P.G. Moerman, J. Groenewold, Y.-J. Chiu, W.K. Kegel, A. van Blaaderen, L.D. Zarzar, Predator–prey interactions between droplets driven by non-reciprocal oil exchange, Nat. Chem. 12 (2020) 1136–1142.

[34] C.M. Wentworth, A.C. Castonguay, P.G. Moerman, C.H. Meredith, R.V. Balaj, S. I. Cheon, L.D. Zarzar, Chemically tuning attractive and repulsive interactions between solubilizing oil droplets, Angew. Chem. Int. Ed. 134 (2022) e202204510.

[35] B.V. Hokmabad, J.A. Canalejo, S. Saha, R. Golestanian, C.C. Maass, Chemotactic self-caging in active emulsions, PNAS 119 (24) (2022), https://doi.org/10.1073/pnas.2122269119 e2122269119.

[36] K. Sasaki, Y. Ishiwatari, K. Ueno, T. Kojima, T. Banno, N. Arai, Molecular modelling of active oil droplet propulsion: Insights from dissipative particle dynamics simulation, Chem. Phys. Lett. 857 (2024) 141680.

[37] H. Kuhn, H. Rehage, Molecular orientation of monododecyl pentaethylene glycol at water/air and water/oil interfaces. A molecular dynamics computer simulation study, Colloid Polym. Sci. 278 (2000) 114–118.

[38] H.-Y. Cai, Y. Zhang, Z.-Y. Liu, J.-G. Li, Q.-T. Gong, Q. Liao, L. Zhang, S. Zhao, Molecular dynamics simulation of binary betaine and anionic surfactant mixtures at decane -Water interface, J. Mol. Liq. 266 (2018) 82–89.

[39] P. Müller, D.J. Bonthuis, R. Miller, E. Schneck, Ionic surfactants at air/water and oil/water interfaces: A comparison based on molecular dynamics simulations, J. Phys. Chem. B 125 (2021) 406–415.

[40] T. Tomonaga, S. Tenma, H. Watanabe, Diffusion of cyclohexane and cyclopentane derivatives in some polar and non-polar solvents. Effect of intermolecular and intramolecular hydrogen-bonding interactions, J. Chem. Soc., Faraday Trans.9 92 (1996) 1863–1867.

[41] T. Takamuku, D. Nishiyama, M. Kawano, F.-A. Miannay, A. Idrissi, Solvation structure and dynamics of coumarin 153 in an imidazolium-based ionic liquid with chloroform, benzene, and propylene carbonate, PCCP 25 (2023) 9868–9880.